

Comparison the stresses and deflections of an isotropic and orthotropic rectangular plates with central circular hole under tension load

Ahmed M. Abdullah

Assistant Lecturer

College of Engineering / University of Mosul

ABSTRACT

The distributions of stresses and deflection in rectangular isotropic and orthotropic plates with central circular hole under transverse static loading have been studied using finite element method. The object of this present work is to analyze the effect of D/Y ratio (where D is hole diameter and Y is plate width) upon stress distribution and deflection in plates under tension subjected to a static loading. The D/Y ratio is varied from (0.1) to (0.9). The results are obtained for four different boundary conditions. The variations of stresses and deflections with respect to D/Y ratio are presented in graphical form. The finite element formulation is carried out by using the analysis section of the ANSYS package

Keywords: Finite Element, Isotropic and orthotropic plates, Boundary conditions.

مقارنة الإجهادات والانحرافات في قطعتين معدنيتين مستطيلتين إحداهما موحدة الخواص والأخرى غير موحدة الخواص ذواتي ثقب مركزي تحت تأثير قوة الشد

أحمد محمود عبدالله

مدرس مساعد

كلية الهندسة / جامعة الموصل

الخلاصة

لقد تم استخدام طريقة العنصر المحدد في دراسة توزيع الاجهادات والانحرافات الحاصلة في قطعتين مستطيلتين الشكل تحتويان على ثقب مركزي من معدنين ذوي خواص غير متساوية تحت تأثير حمل شد ثابت. الغرض من هذا البحث معرفة تأثير قطر الثقب المركزي الموجود في هاتين القطعتين على تركيز الاجهادات فيها وكذلك على الانحرافات التي تحدث فيهما بسبب هذا الحمل ولكل من القطعتين. إن النسبة D/Y (قطر الثقب إلى العرض) تغيرت ما بين (0,1) إلى (0,9) وتم الحصول على النتائج لكلا القطعتان. وقد تم عرض المنحنيات الخاصة بتغير مركز الاجهادات نسبة إلى تغيير D/Y ومناقشتها باستخدام احد برامج العنصر المحدد وهو البرنامج المسمى "ANSYS 12".

الكلمات المفتاحية : العنصر المحدد، قطع موحدة وغير موحدة الخواص، الشروط الحدية.

1. Introduction

Rectangular isotropic or orthotropic plate with central circular hole under transverse static loading, have found widespread applications in various fields of engineering such as aerospace, marine, automobile and mechanical application. For design of plates with hole, accurate knowledge of deflection, stresses and stress concentration is required. Stress concentration arises from any abrupt change in geometry of plate under loading. As a result, stress distribution is not uniform throughout the cross section. Failures (as we know) such as fatigue cracking and plastic deformation frequently occur at points of stress concentration. Wu and Cheng [1] considered a circular hole in a laminated composite material under extensional loading. Chen and Hsu [2] studied the stress concentrations around undulating cracks located at the interface of the two materials. Two sets of analytic functions were used for the two materials and the unevenness of the cracks was modeled using perturbation. Wang and Hasebe [3] studied bending of a plate with an inclusion and a crack. Chaudhuri [4] worked on stress concentration around a part through hole weakening a laminated plate by finite element method. Ishikawa and Kohno [5] used this transformation to determine the stresses around square openings and inclusions for plates under in-plane extension. Paul and Rao [6,7] presented a theory for evaluation of stress concentration factor of thick and FRP laminated plate with the help of Lo Christensen-Wu higher order bending theory under transverse loading. Shastry and Raj [8] have analyzed the effect of fiber orientation for a unidirectional composite laminate with finite element method by assuming a plane stress problem under in plane static loading. Xiwu et al. [9,10] evaluated stress concentration of finite composite laminates with elliptical hole and multiple elliptical holes based on classical laminated plate theory. Iwaki [11] worked on stress concentrations in a plate with two unequal circular holes. Ukadgaonker and Rao [12] proposed a general solution for stresses around holes in symmetric laminates by introducing a general form of mapping function and an arbitrary biaxial loading condition in to the boundary conditions. Ting et al. [13] presented a theory for stress analysis by using rhombic array of alternating method for multiple circular holes. Pan et al. (14) developed a 3D boundary element formulation for the analysis of composite laminates with holes. They used a special Green's function, which satisfies the continuity equation between the lamina, and the free surface on the top and bottom faces to convert the problem to a two-dimensional formulation to avoid discretization in the plate thickness direction.

2. Objectives of this research

In this work, the effect of D/Y ratio on stresses in rectangular isotropic and orthotropic plates under tension load is studied. The purpose of this work is to investigate the effect of D/Y ratio on normal stress in X,Y,Z directions (σ_x , σ_y , σ_z), shear stress in XY, YZ, XZ planes (τ_{xy} , τ_{yz} , τ_{xz}) and on deflection in all direction. These results for different ratios of D/Y are compared for isotropic and orthotropic materials. The results are obtained for four different boundary conditions. The analytical method for such problem is very difficult and hence the finite element method adopt for whole analysis.

3. Theoretical backgrounds

Hooke's law for a homogeneous orthotropic plane stress body is [3]

$$\varepsilon = [S] \{\sigma\} \quad \text{-----} \quad (1)$$

Where S_{11} , S_{12} , & S_{66} , are elastic compliances. In the absence of body forces, the equilibrium equations are

$$\frac{\partial \sigma_x}{\partial x} + \frac{\partial \tau_{xy}}{\partial y} = 0 \text{ and } \frac{\partial \tau_{xy}}{\partial x} + \frac{\partial \sigma_y}{\partial y} = 0 \quad \text{-----} \quad (2)$$

Equation (2) can be satisfied by introducing a stress function, $F(x, y)$, such that

$$\sigma_x = \frac{\partial^2 F}{\partial y^2}, \sigma_y = \frac{\partial^2 F}{\partial x^2} \text{ and } \tau_{xy} = -\frac{\partial^2 F}{\partial x \partial y} \quad \text{-----} \quad (3)$$

The compatibility equation is

$$\frac{\partial^2 \varepsilon_x}{\partial y^2} + \frac{\partial^2 \varepsilon_y}{\partial x^2} = \frac{\partial^2 \gamma_{xy}}{\partial x \partial y} \quad \text{-----} \quad (4)$$

Combining equations (1), (3) and (4) gives the compatibility equation in terms of F . That

equation can be solved using $D_1 D_2 D_3 D_4 F = 0$, where $D_l = (\frac{\partial}{\partial y} - \mu_l \frac{\partial}{\partial x})$ and

$\mu_l (l = 1, 2, 3, 4)$ are the roots of the following characteristic equation [3]:

$$\text{Thus, } s_{11}\mu^4 - 2s_{16}\mu^3 + (2s_{12} + s_{66})\mu^2 - 2s_{26}\mu + s_{22} = 0 \quad \text{-----} \quad (5)$$

In terms of the complex variables $z_1 = x + \mu_1 y$ and $z_2 = x + \mu_2 y$, the stresses of equation (3) can be written as [3]

$$\begin{aligned} \sigma_x &= 2 \operatorname{Re}[\mu_1^2 \phi'(z_1) + \mu_2^2 \psi'(z_2)], \\ &= 2 \operatorname{Re}[\mu_1^2 \frac{\phi'(\zeta_1)}{\omega_1'(\zeta_1)} + \mu_2^2 \frac{\psi'(\zeta_2)}{\omega_2'(\zeta_2)}], \end{aligned}$$

$$\begin{aligned} \sigma_y &= 2 \operatorname{Re}[\phi'(z_1) + \psi'(z_2)], \\ &= 2 \operatorname{Re}[\frac{\phi'(\zeta_1)}{\omega_1'(\zeta_1)} + \frac{\psi'(\zeta_2)}{\omega_2'(\zeta_2)}], \end{aligned}$$

$$\begin{aligned} \sigma_{xy} &= -2 \operatorname{Re}[\mu_1 \phi'(z_1) + \mu_2 \psi'(z_2)], \\ &= -2 \operatorname{Re}[\mu_1 \frac{\phi'(\zeta_1)}{\omega_1'(\zeta_1)} + \mu_2 \frac{\psi'(\zeta_2)}{\omega_2'(\zeta_2)}] \quad \text{-----} \quad (6) \end{aligned}$$

where Φ and ψ are the complex stress potentials. In the absence of rigid body motions, the displacements are

$$\begin{aligned} u &= 2 \operatorname{Re}[p_1 \phi'(z_1) + p_2 \psi'(z_2)], \\ &= 2 \operatorname{Re}[p_1 \phi'(\zeta_1) + p_2 \psi'(\zeta_2)], \end{aligned}$$

$$\begin{aligned} v &= 2 \operatorname{Re}[q_1 \phi'(z_1) + q_2 \psi'(z_2)], \\ &= 2 \operatorname{Re}[q_1 \phi'(\zeta_1) + q_2 \psi'(\zeta_2)], \quad \text{-----} \quad (7) \end{aligned}$$

Where,

$$p_1 = s_{11}\mu_1^2 + s_{12} - s_{16}\mu_1, \quad p_2 = s_{11}\mu_2^2 + s_{12} - s_{16}\mu_2 \quad \text{and}$$

$$q_1 = s_{12}\mu_1 + \frac{s_{22}}{\mu_1} - s_{26}, \quad q_2 = s_{12}\mu_2 + \frac{s_{22}}{\mu_2} - s_{26}$$

4. Description of Problem:

To study the influence of D/Y ratio upon the deflection and the distribution of different stresses, a rectangular plate of (200 mm *100 mm *3 mm) in the directions of X, Y, Z respectively with a circular hole of diameter D at the centre is selected. This plate is exposed to a uniformly distributed static load $P = (5) \text{ N}$ in tension. The results of all cases are analyzed using finite element method. Figure (1) shows the basic model of the problem and its main axes. The D/Y ratio is varied from (0.1) to (0.9). Following Table (1). Where; E, G and μ represent modulus of elasticity, modulus of rigidity and Poisson's ratio respectively.

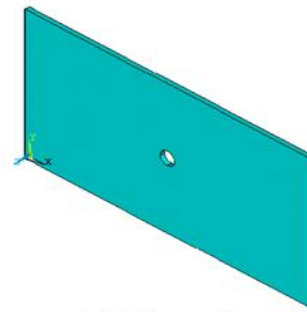


Fig. 1 Basic model of the problem

Table (1): Material properties which are used in the analysis.

Properties	Isotropic	Orthotropic
Ex	225 GPa	225 GPa
Ey	-----	127 GPa
Ez	-----	127 GPa
μ_{xy}	-----	0.3
μ_{yz}	-----	0.3
μ_{zx}	-----	0.3
Gxy	37 GPa	37 GPa
Gyz	-----	37 GPa
Gzx	-----	37 GPa

5. Finite Element Analysis

Twenty noded Structural 3-D Solid Element (specified as Solid95 in ANSYS package) with element length of 2 mm, is selected based on convergence test and used through out the study. Each node has six degrees of freedom, making a total of 48 degrees of freedom per element. In order to construct the graphical image of the geometries of models for different D/Y ratios, rectangular isotropic and orthotropic plates examined using the ANSYS (Advanced Engineering Simulation). Mapped meshing are used for all models so that more elements are employed near the hole boundary. Due to the symmetric nature of different models investigated, it is necessary to discretize the quadrant plate for finite element analysis. Main task in finite element analysis is the selection of the suitable element type. Numbers of checks and convergence test is made to select of suitable element type from out the different available elements and to decide the element length required. Figure (2) provides the example of the discretized models for D/Y = (0.2), used in study.

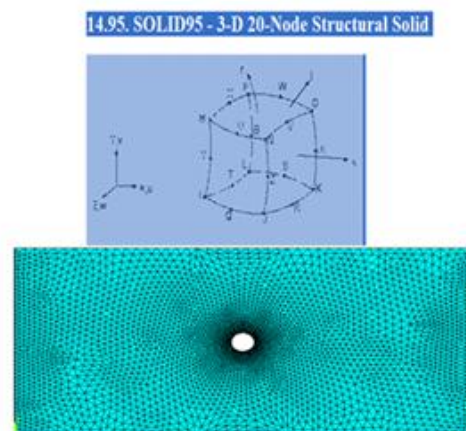


Fig. 2 Typical example of finite element model for D/Y = (0.2)

6. ANSYS

ANSYS finite element analysis software enables engineers to perform the important tasks. Build computer models or transfer computer Aided Drafting (CAD) models of structures, products, components, or systems. Apply operating loads or other design performance conditions and study the physical responses, such as stress levels, temperature distributions, or the impact of electromagnetic fields. Optimize a design early in the development process to reduce production costs [15]. Prototype testing in environments can be done where it otherwise would be undesirable or impossible. The ANSYS program has a comprehensive graphical user interface (GUI) that gives wide facilities, interactive access to program function, commands, documentation, and reference material. The menu system helps users navigate through the ANSYS program. Users can put the required data and by using the mouse and the keyboard or both combinations.

7. Results and Discussion

Numerical results are presented for isotropic and orthotropic rectangular plates with a central circular hole. The material properties of different used materials are shown in table (1). Where; E, G and μ represent modulus of elasticity, modulus of rigidity and Poisson's ratio respectively. Four different plates with different boundary conditions (A), (B), (C) and (D) are tasted. In plate (A) all edges are fixed, in plate (B); two edges are fixed and other two are simply, in plate (C) all edges (in other sides) are fixed and in plate (D); two edges (in other sides) are fixed and other two are simply. Figure (3) provides the boundary conditions at all edges of plates (A), (B), (C) and (D). Stresses and deflections are obtained for uniformly distributed loads $P = (5) \text{ N}$ for all cases and for (D/Y) ratios from (0.1) to (0.9). The stresses and deflection in all directions for full plate (A), (B), (C) and (D), made of different materials under uniformly distributed load of (5) N are listed in

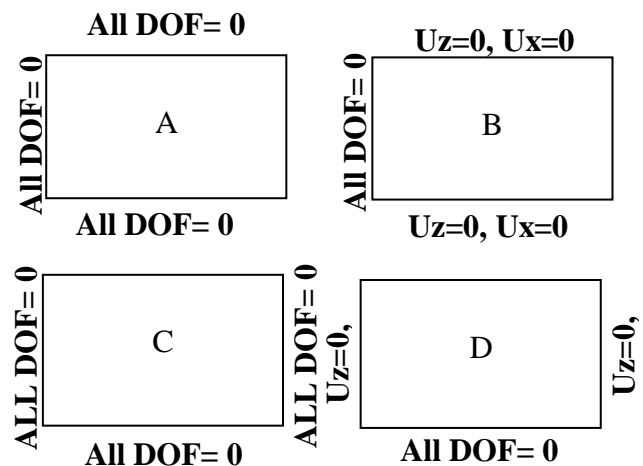


Fig. 3 Boundary conditions for all edges of plates (A), (B), (C) and (D)

Tables (2), show the effect of D/Y ratio on (σ_x , σ_y , σ_z , U_x , U_y and U_z) and (τ_{xy} , τ_{yz} , τ_{xz} , σ_{Von} and U_{sum}) in plates (A), (B), (C) and (D) of full plate (without hole) for isotropic and orthotropic materials.

Tables (2): Stresses and deflection for full plate.

Material Type	Plate	σ_x (MPa)	σ_y (MPa)	σ_z (MPa)	U_x (μm)	U_y (μm)	U_z (μm)	τ_{xy} (MPa)	τ_{yz} (MPa)	τ_{xz} (MPa)	σ_{Von} (MPa)	U_{sum} (μm)
Isotropic	(A)	2.8	1.27	.240	.443	.089	.008	2.15	.128	.865	5.00	.443
	(B)	2.28	1.71	.210	.507	.221	.010	1.06	.168	.874	2.64	.507
	(C)	.418	1.28	.294	.053	.300	.011	.872	.525	.117	2.24	.301
	(D)	.795	1.22	.311	.128	.325	.302	.515	.446	.239	1.28	.436
Orthotropic	(A)	2.64	.877	.192	.653	.120	.011	1.40	.101	.775	3.71	.654
	(B)	2.64	1.26	.171	.718	.322	.014	.845	.125	.782	2.72	.718
	(C)	.613	1.29	.261	.076	.597	.917	.755	.498	.120	3.05	1.09
	(D)	1.02	1.27	.277	.196	.643	1.49	.562	.494	.066	1.41	1.62

In figures (4, 5) when there is no hole in the piece ,(plate A), note that when Isotropic is used the value of Von Mises stress is not more than (5) MPa but (under the same conditions) on the other hand when Orthotropic is used the stress will be (3.71) MPa. In figures (6, 7), when ($D / Y = 0.5$) it can be noticed that the value of Von Mises stress changed from (5.18) to (4.23) MPa, whereas in figures (8, 9) at ($D / Y = 0.9$) the value of Von Mises stress decreased from (5.82) to (4.87) MPa.

In figures (10, 11), (plate A) with no hole in the piece, the value of deflection for Isotropic, the value of Displacement vector sum (Usum) is not more than (0.443) μm , but (under the same conditions) in the case of using Orthotropic will be (.654) μm . Where as in figures (12, 13) at ($D / Y = 0.9$) the value of displacement vector sum (Usum) increased from (.553) to (1.05) μm .

In figures (14, 15) (plate C) with no hole in the piece, the value of deflection for Isotropic, is used, the value of Von Mises stress is not more than (2.24) Mpa, but (under the same conditions) in the case of using Orthotropic will be (3.05) Mpa. Whereas in figures (16, 17) at ($D / Y = 0.9$) value of Von Mises stress increased from(10.9)to (12.4) MPa.

In figures (18, 19) (plate C) with no hole in the piece, the value of deflection for Isotropic is used, the value of displacement vector sum (Usum) is not more than (0.301) μm . However (under the same conditions) in the case of Orthotropic will be (1.09) μm , whereas in figures (20, 21) at ($D / Y = 0.9$) the value of Displacement vector sum (Usum) increased from (3.57) to (5.45) μm .

In figure (22) we see that the variation of σ_x with respect to D/Y ratio is remained constant approximately at (2.8) MPa. In case of plate (A) it is decreased to (2.4) MPa at max. D/Y for isotropic but for orthotropic plate it can be noticed that σ_x is about (2.64) MPa firstly then increased to reach a max. Value (3.8) MPa at $D/Y=0.7$ and finally decreased to (2.8) MPa at max. D/Y. In the case (B) it is observed that σ_x is about (2.28) MPa firstly for isotropic and (2.64) MPa for orthotropic, after that it is increased to reach a max. value (2.6) MPa for isotropic and (4.5) for orthotropic at $D/Y=0.9$. In the case of plate (C); σ_x increased from (.418) and (.613) MPa to (10) and (12) MPa for isotropic and orthotropic plates respectively with increasing of D/Y ratio to 0.9. In the case of plate (D); σ_x increased from(.795)and(1.02) MPa to(10.5) and(12.5) MPa for isotropic and orthotropic plates respectively with increase of D/Y ratio to 0.9.

In figure (23), the following observations can be made from these results. It can be noticed that the variation of σ_y with respect to D/Y ratio is observed: the maximum for isotropic plate in the case of plate (C), maximum for both in the case of plate (D), maximum for orthotropic plate in the case of plate (B), and almost negligible in the case of plate (A). In the case of plate (A); σ_y increased from (1.27) and (0.877) MPa to (1.65) and (1.55) MPa with increasing of D/Y ratio to 0.9 for isotropic and orthotropic plates respectively. In case of plate (B); σ_y increased from (1.71) and (1.26) MPa to (3.55) MPa for both with increase of D/Y ratio to 0.9. In case of plate (C); σ_y increased from (1.28) and (1.29) MPa to (4.0) and (3.1) MPa with increasing of D/Y ratio to 0.9 for isotropic and orthotropic plates respectively. In case of plate (D); σ_y increased from (1.22) and (1.27) MPa to (4.02) and (4.08) MPa with increase of D/Y ratio to 0.9 for isotropic and orthotropic plates respectively.

Figure (24) shows the following observations. It can be noticed that the variation of σ_z with respect to D/Y ratio is observed, maximum in the case of plates (C) and (D) for isotropic plates and significant in plates (A) and (B). In plate (A); σ_z increased from (.24) and (.192) MPa, to (.41) and (.321) MPa, with $D/Y = 0.2$, and decreased to (.335) and (.269) MPa, with increase of D/Y ratio from 0.2 to 0.5, and again increased to (.393) and (.314)

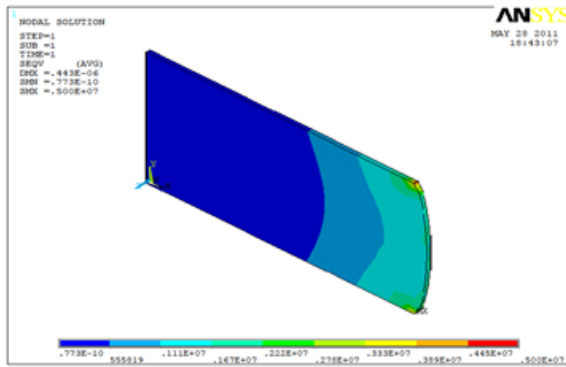


Fig. 4 Stress distribution(Von Mises stresses) for isotropic material (without hole)

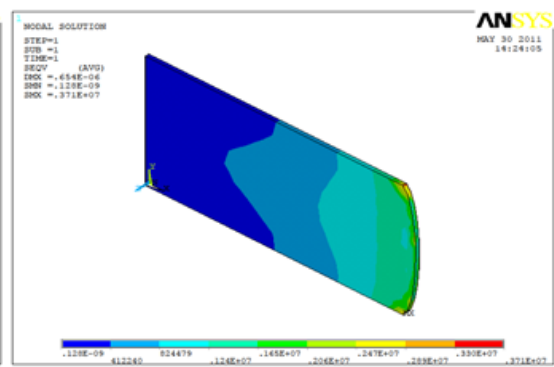


Fig. 5 Stress distribution(Von Mises stresses) for orthotropic material (without hole)

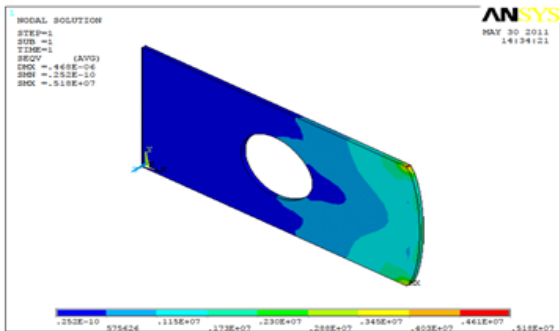


Fig. 6 Stress distribution(Von Mises stresses) for isotropic material (with D/Y ratio = 0.5)

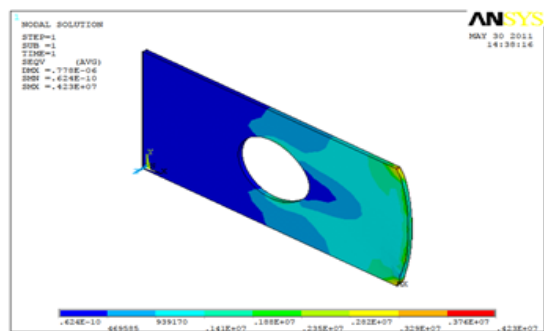


Fig. 7 Stress distribution (Von Mises stresses) for orthotropic material (with D/Y ratio = 0.5)

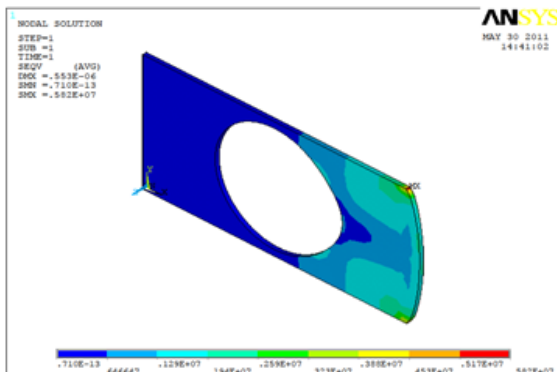


Fig. 8 Stress distribution(Von Mises stresses) for isotropic material (with D/Y ratio = 0.9)

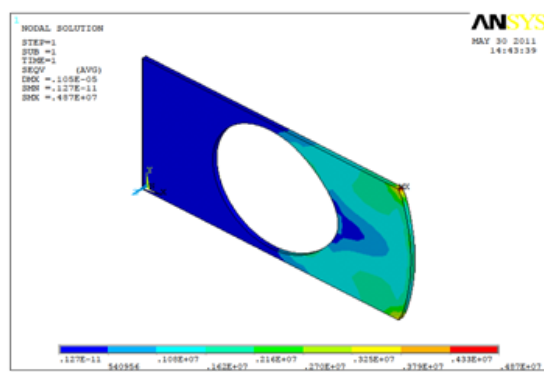


Fig. 9 Stress distribution (Von Mises stresses) for orthotropic material (with D/Y ratio = 0.9)

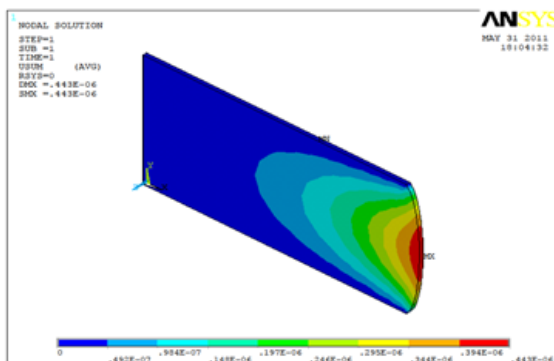


Fig. 10 Deflection distribution (U_{sum}) for isotropic material (without hole)

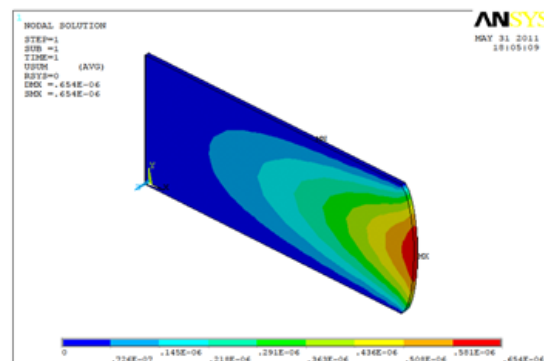


Fig. 11 Deflection distribution (U_{sum}) for orthotropic material (without hole)

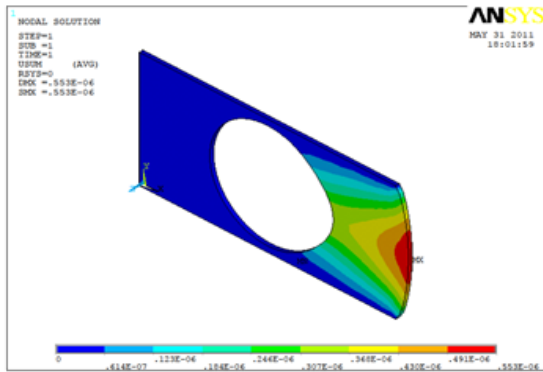


Fig. 12 Deflection distribution (\bar{U}_{SUM}) for isotropic material (with D/Y ratio = 0.9)

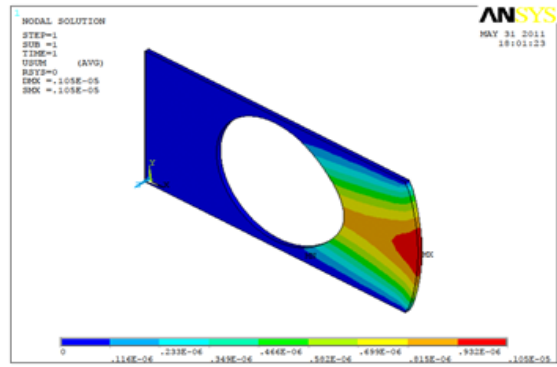


Fig.13 Deflection distribution (\bar{U}_{SUM}) for orthotropic material (with D/Y ratio = 0.9)

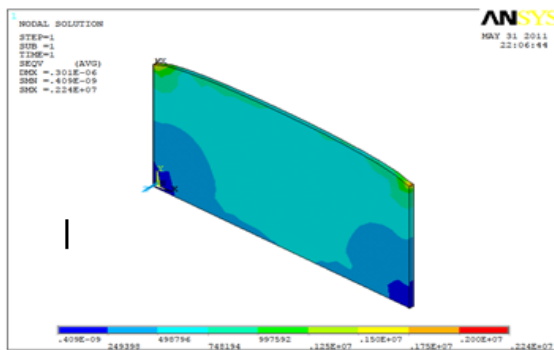


Fig. 14 Stress distribution (Von Mises stress) for isotropic material (without hole) (Horizontal case)

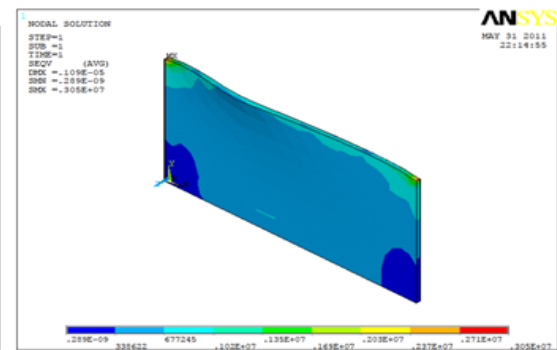


Fig. 15 Stress distribution (Von Mises stress) for orthotropic material (without hole)

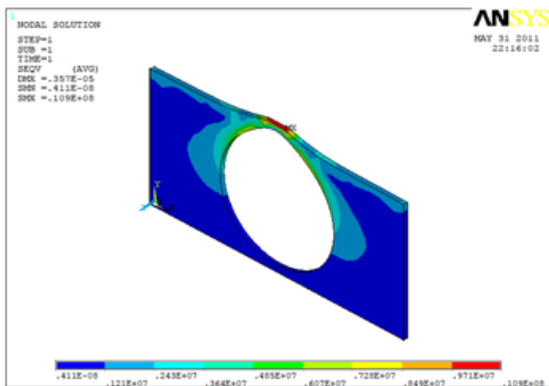


Fig. 16 Stress distribution (Von Mises stress) for isotropic material (with D/Y ratio = 0.9) (Horizontal case)

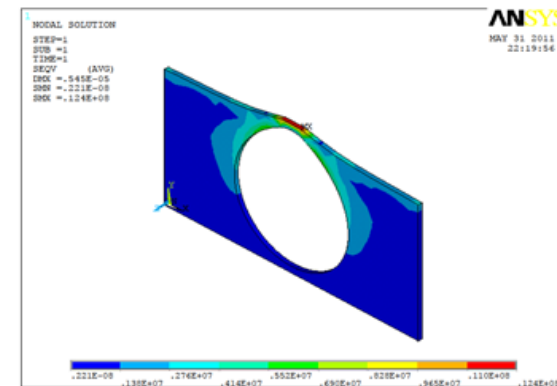


Fig. 17 Stress distribution (Von Mises stress) for orthotropic material (with D/Y ratio = 0.9) (Horizontal case)

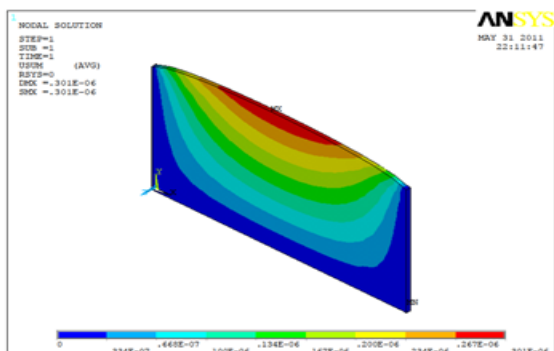


Fig. 18 Deflection distribution (\bar{U}_{SUM}) for isotropic material (without hole) (Horizontal case)

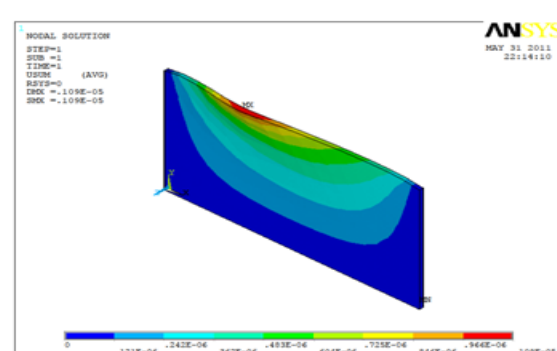


Fig. 19 Deflection distribution (\bar{U}_{SUM}) for orthotropic material (without hole) (Horizontal case)

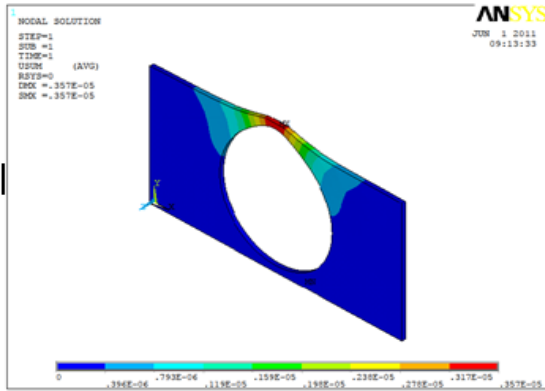


Fig. 20 Deflection distribution (U_{SUM}) for isotropic material (with D/Y ratio = 0.9) (Horizontal case)

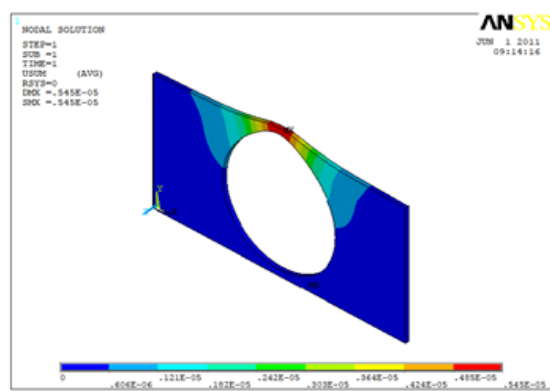


Fig. 21 Deflection distribution (U_{SUM}) for orthotropic material (with D/Y ratio = 0.9) (Horizontal case)

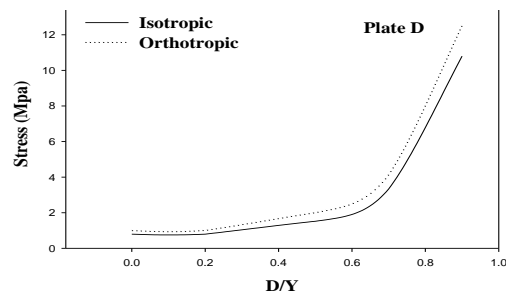
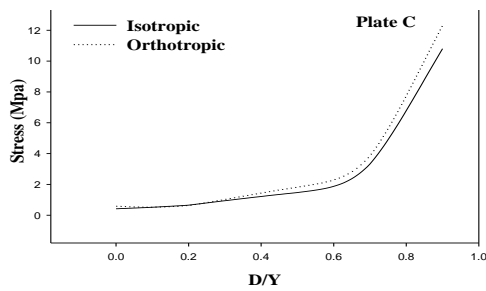
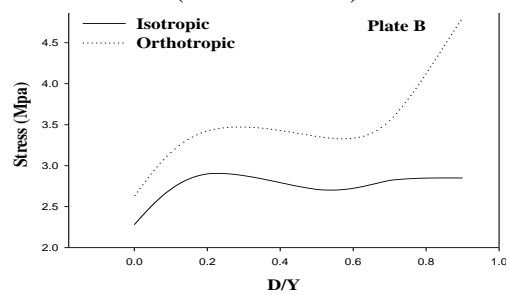
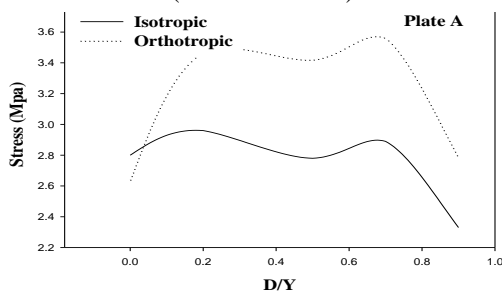


Fig.22 Effect of hole diameter on σ_x in plates (A), (B), (C) and (D) of an isotropic and orthotropic materials

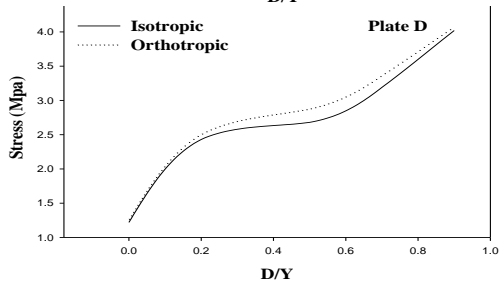
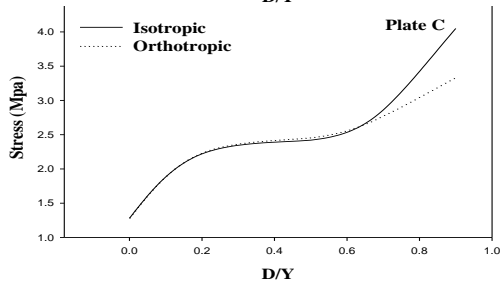
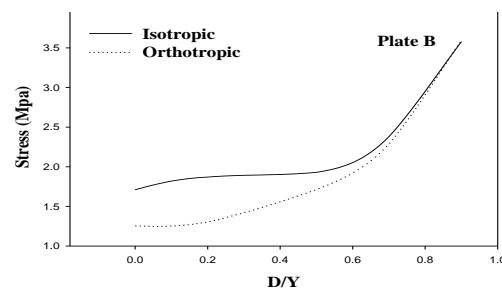
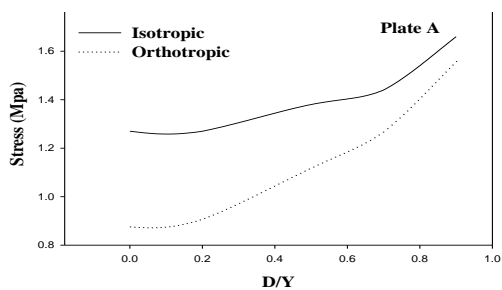


Fig. 23 Effect of hole diameter on σ_y in plates (A), (B), (C) and (D) of an isotropic and orthotropic materials

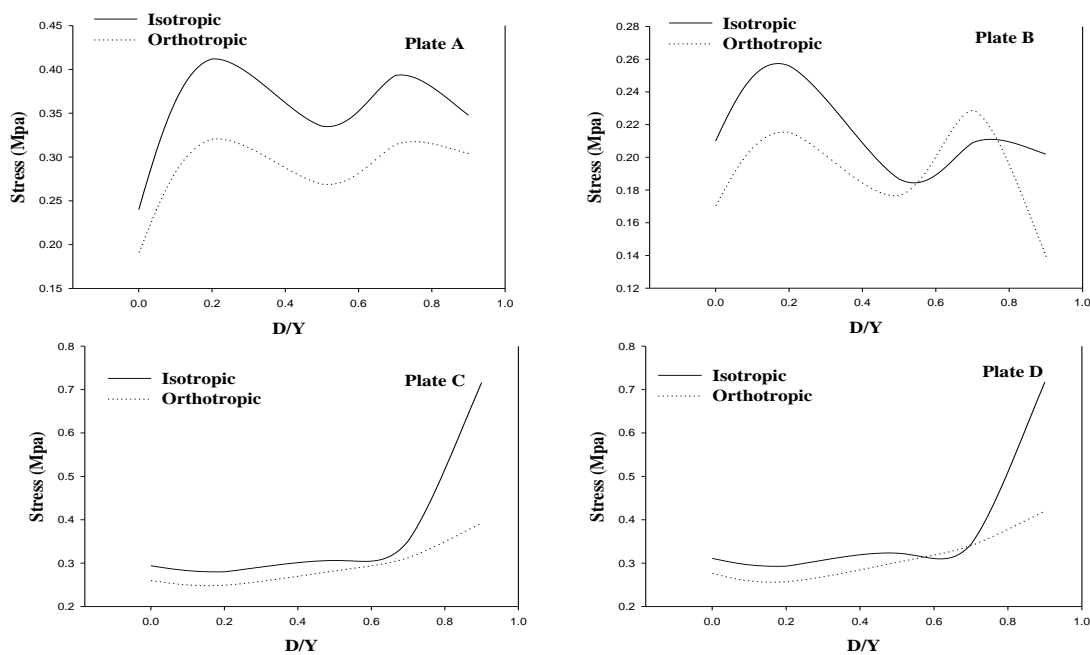


Fig. 24 Effect of hole diameter on σ_z in plates (A), (B), (C) and (D) of an isotropic and orthotropic materials

increase of D/Y ratio from 0.7 to 0.9 for isotropic and orthotropic plates respectively. In the case of plate (B); σ_z increased from (.21) and (.171) MPa to (.256) and (.215) MPa with increase of D/Y ratio from 0.5 to 0.7, and again decreased to (.347) and (.304) MPa, with D/Y = 0.2, decreased to (.186) and (.176) MPa with increase of D/Y ratio from 0.2 to 0.5. Again increased to (.208) and (.229) MPa with increase of D/Y ratio from 0.5 to 0.7 and again decreased to (.201) and (.139) MPa with increase of D/Y ratio from 0.7 to 0.9 for isotropic and orthotropic plates respectively. In the case of plate (C); σ_z increased from (.294) and (.261) MPa to (0.715) and (0.393) MPa with increase of D/Y ratio to 0.9 for isotropic and orthotropic plates respectively. In the case of plate (D); σ_z remained constant (for isotropic plate) approximately at (0.3) MPa until D/Y= 0.7, then increased to (7.25) MPa, whereas it increased from (.277) to (.41) MPa with increase of D/Y ratio to 0.9 for orthotropic plate.

Figure (25) shows the following observations from these results. It can be noticed that the variation of σ_{von} with respect to D/Y ratio is observed, maximum in the case of plates (C) and (D) and significant in the plates (A) and (B) for both plates. In the case of plate (A); σ_{von} increased from (5.0) and (3.7) MPa to (5.82) and (4.87) MPa with increase of D/Y ratio to 0.9 for isotropic and orthotropic plates respectively. In the case of plate (B); σ_{von} increased from (2.64) and (2.72) MPa to (3.66) and (3.69) MPa with D/Y = 0.2, decreased to (3.46) and (3.58) MPa with increase of D/Y ratio from 0.2 to 0.5 and again increased to (4.52) and (4.81) MPa when D/Y = 0.9 for isotropic and orthotropic plates respectively. In the case (C) ; σ_{von} increased from (2.24) and (3.05) MPa to (3.31) and (3.71) MPa with increase of D/Y ratio to 0.7, then increased to (10.9) and (12.4) MPa when D/Y = 0.9 for isotropic and orthotropic plates respectively. In the case of plate (D); σ_{von} increased from (1.28) and (1.41) MPa to (10.9) and (12.6) MPa with increase of D/Y ratio to 0.9 for isotropic and orthotropic plates respectively.

Figure (26) shows the following observations from these results. It can be noticed that the variation of U_x with respect to D/Y ratio is observed. The maximum for both plates in the case of plate (C), and maximum for orthotropic plate, and significant for isotropic plate in the case of plate (B), and significant for orthotropic plates in the case of plates (A) and (B),

and almost negligible for isotropic plates in the case of plates (A) and (B). In the case of plate (A); U_x increased from (.443) and (.653) μm to (.552) and (1.05) μm with increased of D/Y ratio to 0.9 for isotropic and orthotropic plates respectively. In the case of plate (B); U_x increased from (.507) and (.718) μm to (.983) and (1.68) μm with increased of D/Y ratio to 0.9 for isotropic and orthotropic plates respectively. In case of plate (C); U_x increased from (.053) and (.076) μm to (.579) and (.70) μm with increased of D/Y ratio to 0.9 for isotropic and orthotropic plates respectively. In the case of plate (D); U_x increased from (.128) and (.196) μm to (.577) and (.695) μm with increase of D/Y ratio to 0.9 for isotropic and orthotropic plates respectively.

Figure (27) shows the following observations from these results. It can be noticed that the variation of U_y with respect to D/Y ratio is observed, maximum for both plate in the case of plates (C), and (D), and significant for both plates in the case of plate (B), and almost negligible for both plates in the case of plate (A). In the case of plate (A); U_y increased from (.089) and (.12) μm to (.118) and (.209) μm with increase of D/Y ratio to 0.9 for isotropic and orthotropic plates respectively. In the case of plate (B); U_y increased from (.221) and (.322) μm to (.778) and (1.53) μm with increase of D/Y ratio to 0.9 for isotropic and orthotropic plates respectively. In the case of plate (C); U_y increased from (0.3) and (0.597) μm to (3.56) and (5.45) μm with increase of D/Y ratio to 0.9 for isotropic and orthotropic plates respectively. In the case of plate (D); U_y increased from (.325) and (.643) μm to (3.72) and (6.12) μm with increase of D/Y ratio to 0.9 for isotropic and orthotropic plates respectively.

Figure (28) shows the following observations from these results. It can be noticed that the variation of U_z with respect to D/Y ratio is observed, maximum for both plates in the case of plates (C), and (D), minimum for both plates in the case of (B), and significant for orthotropic plate, but negligible for isotropic plate in the case of plate (A). In the case of plate (A); U_z increased for orthotropic plate from (.013) to (.676) μm when D/Y = 0.2, then decreased to (.015) μm , whereas it for isotropic plate approximately remained constant at (.01) μm . In the case of plate (B); U_z increased from (.01) and (.014) μm to (.215) and (.259) μm with D/Y = 0.2, then decreased to (.011) and (.021) μm with increase of D/Y ratio from 0.2 to 0.7 and again increased to (.013) and (.023) μm when D/Y = 0.9 for isotropic and orthotropic plates respectively. In the case of plate (C); U_z increased from (.301) and (1.09) μm to (3.57) and (5.45) μm with increase of D/Y ratio to 0.9 for isotropic and orthotropic plates respectively. In the case of plate (D); U_z decreased from (.302) and (.215) μm to (.010) and (.015) μm with D/Y = 0.7, then increased to (.028) and (.045) μm with increase of D/Y ratio from 0.7 to 0.9 for isotropic and orthotropic plates respectively.

Figure (29) shows the following observations from these results. It can be noticed that the variation of U_{sum} with respect to D/Y ratio is maximum for both plates in the case of plates (C), and (D), and significant for orthotropic plates in the case of plates (A) and (B), and almost negligible for isotropic plates in the case of plates (A) and (B). In the case of plate (A); U_{sum} increased from (.443) and (.654) μm to (.553) and (1.05) μm with increase of D/Y ratio to 0.9 for isotropic and orthotropic plates respectively. In the case of plate (B); U_{sum} increased from (.507) and (.718) μm to (.984) and (1.86) μm with increase of D/Y ratio to 0.9 for isotropic and orthotropic plates respectively. In the case of plate (C); U_{sum} increased for isotropic plate from (.306) to (.405) μm . It decrease for orthotropic plate from (1.09) to (.636) μm , when D/Y = 0.2, then increased for both plate from (.405) and (.636) to (3.57) and (5.45) μm with increase of D/Y ratio from 0.2 to 0.9 for isotropic and orthotropic plates respectively. In the case of plate (D); U_{sum} increased for isotropic plate from (.436) to (.467) μm . It decrease for orthotropic plate from (1.62) to (.68) μm when D/Y = 0.2, then increased

for both plate from (.467) and (.68) to (3.72) and (6.12) μm with increase of D/Y ratio from 0.2 to 0.9 for isotropic and orthotropic plates respectively.

Figure (30), cases of plate, the variation of τ_{yz} with respect to D/Y ratio is negligible in the four cases of plates, the variation of τ_{xz} with respect to D/Y ratio is observed, significant in case of plate (A), maximum in the case of plate (B) and negligible in the cases of (C) and (D). In the case (A) the value of τ_{xy} , increased from (2.17) to (2.64) MPa, and τ_{yz} increased from (.128) to (.212) MPa, with increase of D/Y ratio to 0.9. And τ_{xz} increased from (.888) to (1.27) MPa, when D/Y = 0.2, then decreased to (1.2) MPa with increase of D/Y ratio from 0.2 to 0.5, then, increased to (1.24) MPa with increase of D/Y ratio from 0.5 to 0.7, and finally decreased to (.966) MPa, with increase of D/Y ratio from 0.7 to 0.9. In the case (B) the value of τ_{xy} increased from (1.09) to (1.6) MPa, and τ_{yz} increased from (.174) to (.334), when D/Y = 0.2. Then decreased to (.19) MPa with increase of D/Y ratio from 0.2 to 0.9. And τ_{xz} increased from (.902) to (1.29) MPa, when D/Y = 0.2, then decreased to (1.23) MPa, with increase of D/Y ratio from 0.2 to 0.5. Then increased to (1.27) MPa with increase of D/Y ratio from 0.5 to 0.7, and decreased to (.984) MPa with increase of D/Y ratio from 0.7 to 0.9. In the case (C) the value of τ_{xy} increased from (.872) to (3.69) MPa, with increase of D/Y ratio to 0.9. And τ_{yz} decreased from (.525) to (.445) MPa when D/Y = 0.2, then increased to (.663) MPa with increase of D/Y ratio from 0.2 to 0.7. And finally decreased to (.651) MPa with increase of D/Y ratio from 0.7 to 0.9, and τ_{xz} increased from (.154) to (.439) MPa when D/Y = 0.5, then decreased to (.14) MPa with increase of D/Y ratio from 0.5 to 0.9, then increased to (.327) MPa with increase of D/Y ratio from 0.7 to 0.9. In the case (D) the value of τ_{xy} increased from (.515) to (3.55) MPa, with increase of D/Y ratio to 0.9 and τ_{yz} decreased from (.446) to (.432) MPa, when D/Y = 0.2, then increased to (.646) MPa with increase of D/Y ratio from 0.2 to 0.7. Finally decreased to (.617) MPa, with increase of D/Y ratio from 0.7 to 0.9, and τ_{xz} decreased from (.239) to (.028) MPa, when D/Y = 0.2, then increased to (.038) MPa, with increase of D/Y ratio from 0.2 to 0.5, and decreased to (.032) MPa with increase of D/Y ratio from 0.5 to 0.7, and finally increased to (.356) MPa with increase of D/Y ratio from 0.7 to 0.9.

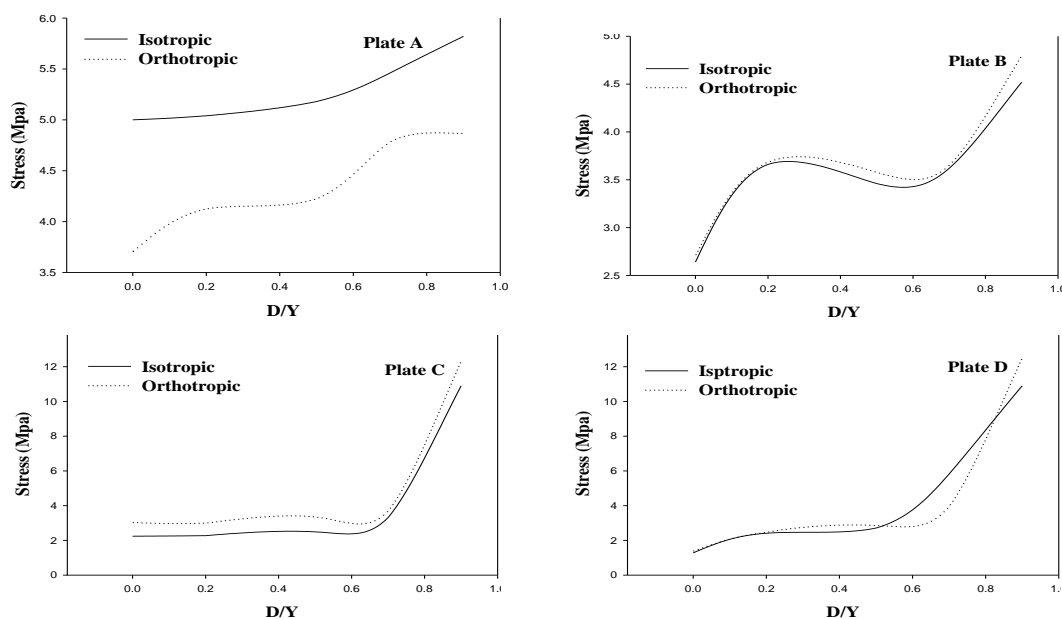


Fig. 25 Effect of hole diameter on σ_{von} in plates (A), (B), (C) and (D) of an isotropic and orthotropic materials

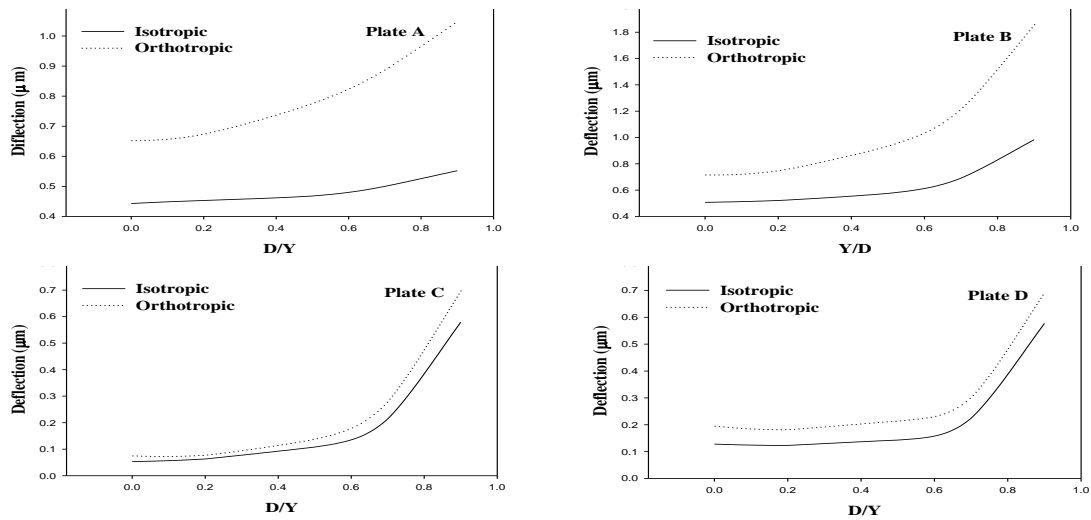


Fig.26 Effect of hole diameter on U_x in plates (A), (B), (C) and (D) of isotropic and orthotropic materials

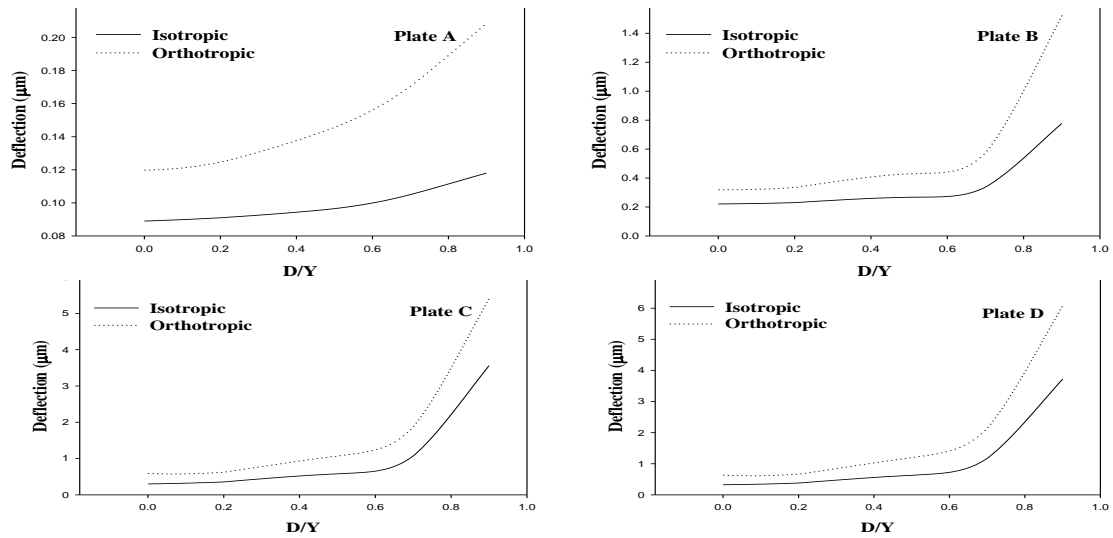


Fig.27 Effect of hole diameter on U_y in plates (A), (B), (C) and (D) of isotropic and orthotropic materials

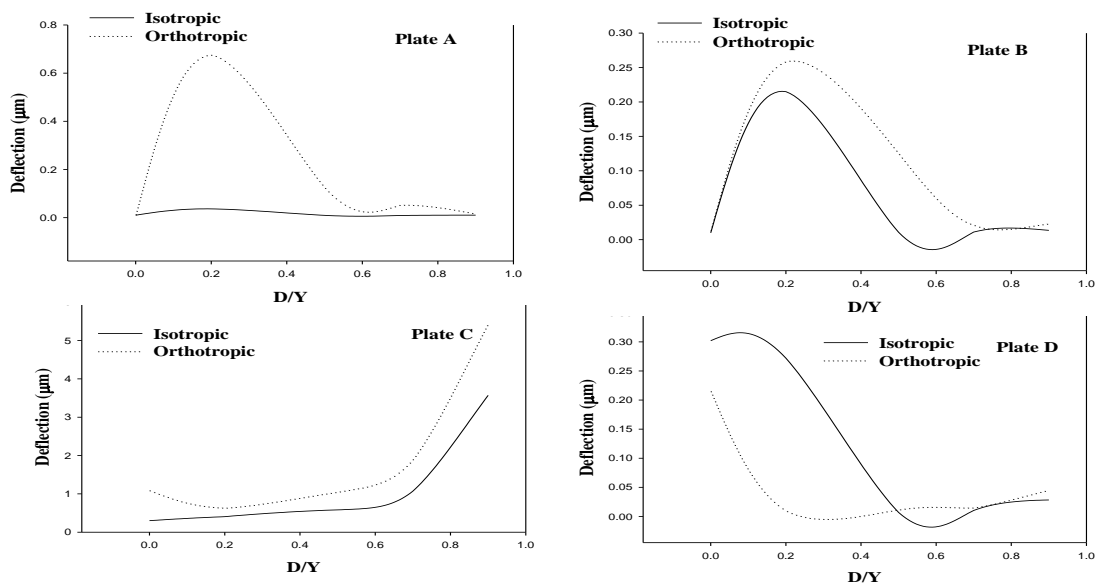


Fig.28 Effect of hole diameter on U_z in plates (A), (B), (C) and (D) of isotropic and orthotropic materials

Figure (31), shows the following observations from these results. In the case of orthotropic materials, it can be noticed that, the variation of τ_{xy} with respect to D/Y is maximum in the four cases of plate. And the variation of τ_{yz} with respect to D/Y ratio is negligible in the four cases of the plate, and the variation of τ_{xz} with respect to D/Y ratio is observed: significant in the case of plate (A), and maximum in the case of plate (B), and negligible in the cases of (C) and (D). In the case (A) the value of τ_{xy} , increased from (1.4) to (1.79) MPa, with increase of D/Y ratio to 0.9. And τ_{yz} increased from (.101) to (.239) MPa increase of D/Y ratio from 0.2 to 0.7, then decreased to (.184) MPa with increase of D/Y ratio from 0.7 to 0.9 and τ_{xz} increased from (.775) to (1.03) MPa when D/Y = 0.2, then decreased

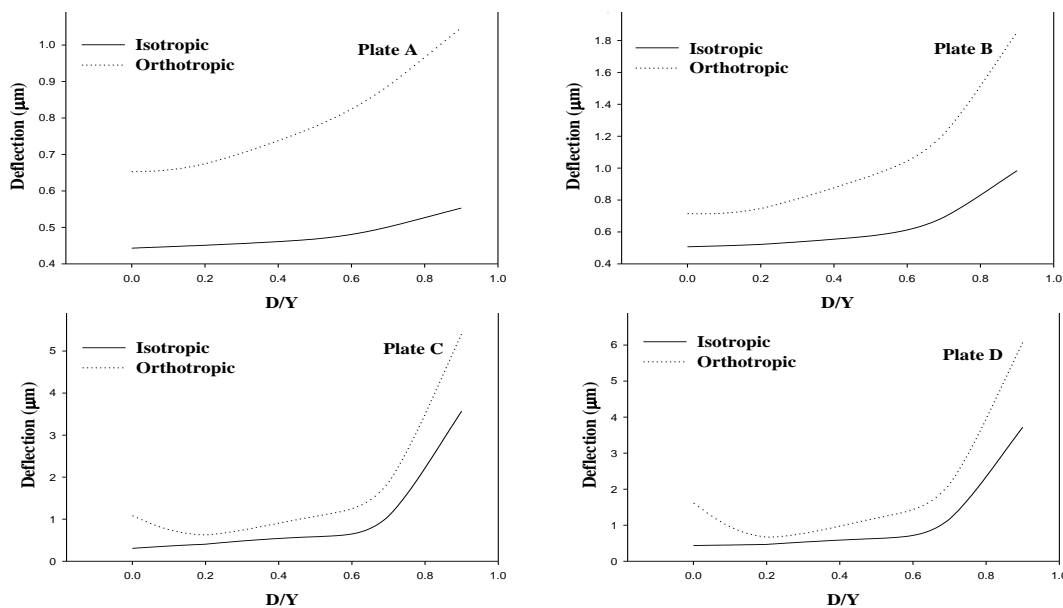


Fig.29 Effect of hole diameter on USUM in plates (A), (B), (C) and (D) of isotropic and orthotropic materials

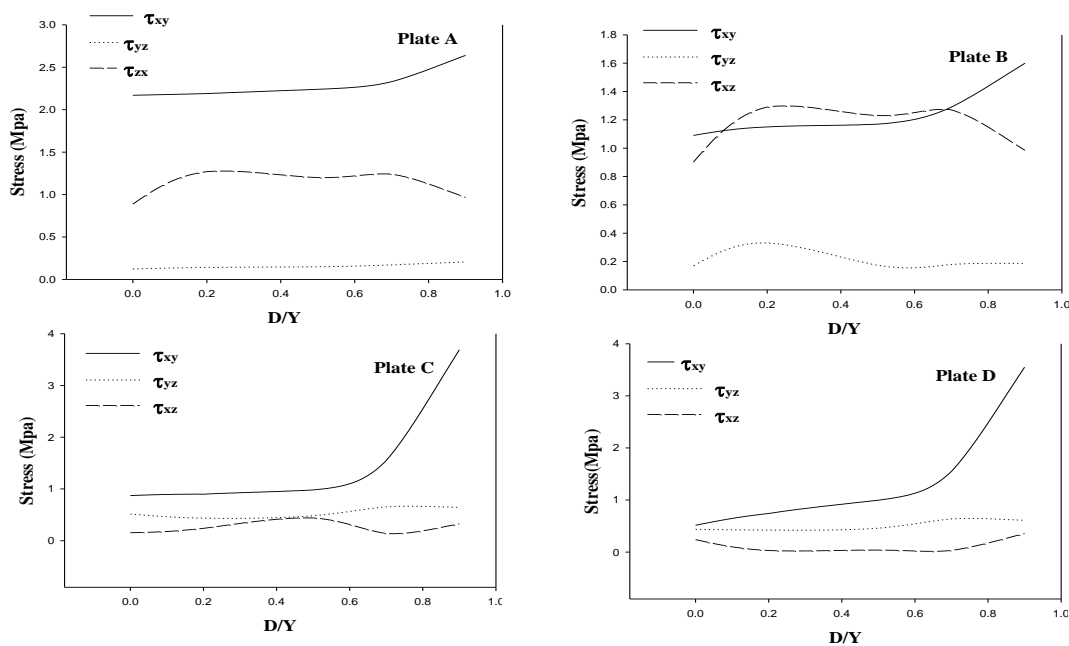


Fig.30 Effect of hole diameter on τ_{xy} , τ_{yz} , and τ_{xz} in plates (A), (B), (C) and (D) of an isotropic material

to (.869) MPa with increase of D/Y ratio from 0.2 to 0.9. In the case (B) the value of τ_{xy} increased from (.845) to (1.43) MPa, with increase of D/Y ratio to 0.9. In addition, τ_{yz} increased from (.125) to (.119) MPa, with increase of D/Y ratio from 0.2 to 0.7. Then decreased to (.137) MPa with increase of D/Y ratio from 0.7 to 0.9 and τ_{xz} increased from (.782) to (1.04) MPa when D/Y = 0.2, then decreased to (.871) MPa with increase of D/Y ratio from 0.2 to 0.9. In the case (C) the value of τ_{xy} increased from (.755) to (3.06) MPa, with increase of D/Y ratio to 0.9. In addition, τ_{yz} decreased from (.494) to (.42) MPa, when D/Y = 0.2. Then increased to (.62) MPa, with increase of D/Y ratio from 0.2 to 0.7, then decreased to (.591) MPa with increase of D/Y ratio from 0.7 to 0.9 and τ_{xz} decreased from (.12) to (.09) MPa when D/Y = 0.2, then increased to (.306) MPa with increase of D/Y ratio from 0.2 to 0.9. In the case (D) the value of τ_{xy} increased from (.562) to (3.08) MPa, with increase of D/Y ratio to 0.9. In addition, τ_{yz} decreased from (.498) to (.423) MPa when D/Y = 0.2, then increased to (.63) MPa with increase of D/Y ratio from 0.2 to 0.7. In addition, decreased to (.604) MPa with increase of D/Y ratio from 0.7 to 0.9 and τ_{xz} decreased from (.066) to (.026) MPa when D/Y = 0.2, then increased to (.329) MPa with increase of D/Y ratio from 0.2 to 0.9.

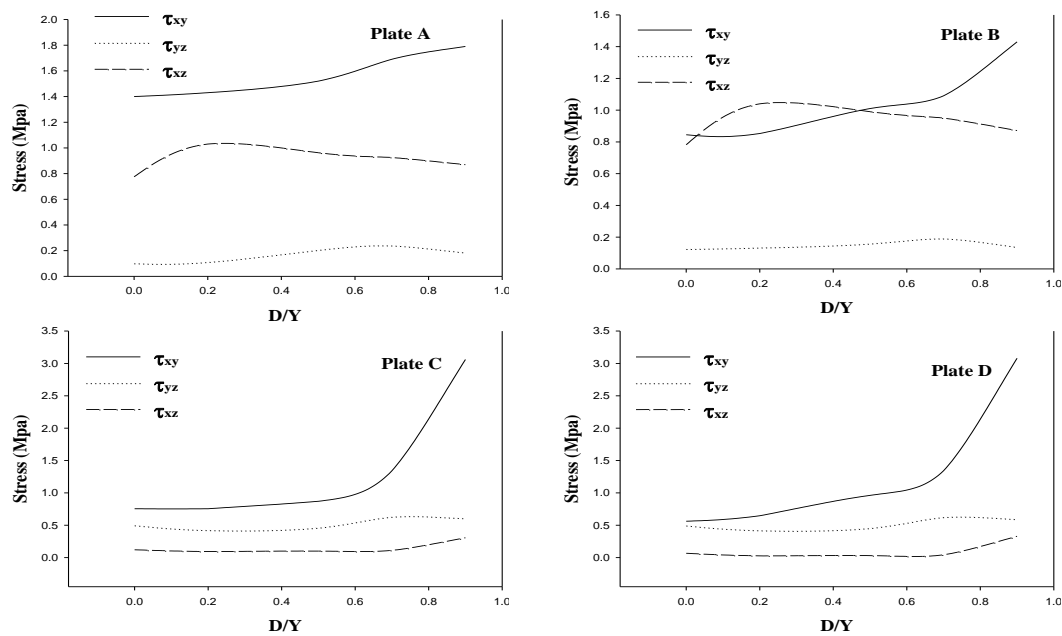


Fig.31 Effect of hole diameter on τ_{xy} , τ_{yz} , and τ_{xz} in plates (A), (B), (C) and (D) of an orthotropic material

8. Conclusion

The variation of the stresses (σ_x) with respect to D/Y ratio was clearly observed in orthotropic plates, compared to isotropic plates for all boundary conditions. For (a) and (b), the variation of the stresses (σ_y) with respect to D/Y ratio is small when considered orthotropic material as compared to that when isotropic, whereas on the same variants is more for plate (D). When (D/Y = 0.7), the variations are the same. After that, it increases for plate (C) when isotropic. The variation is observed of the stresses (σ_z), with respect to D/Y ratio, is less than in when orthotropic than that when isotropic for all boundary conditions, especially when D/Y becomes 0.7. When orthotropic, the variation of the stress σ_{Von} for (A)

and (C) is less than that when isotropic especially when D/Y becomes 0.7. After that, the two materials coincide at the same path for both (B) and (D).

The variation of the deflections (U_x), (U_y) with respect to D/Y ratio was clearly observed in orthotropic plates as compared to isotropic plates for all boundary conditions. For all cases, developed maximum deflection in x- direction (U_x), whereas the minimum deflection (U_x) was developed in plate (A). Plate (D) developed maximum deflection in y- direction (U_y) and plate (A) developed the minimum. For all, the deflections in both directions increased at D/Y = 0.7.

The variation observed of the deflection (U_z) for orthotropic, with respect to D/Y ratio, is greater than that for isotropic plates in all boundary conditions except (D). For both materials, the maximum deflection in z- direction is observed in plate (C). For all materials, plates (A) and (B) developed increasing in deflection (U_z) with D/Y ratio for the first time, then the deflection decreased. In the case of plate (D) the deflection (U_z) decreased with increasing of D/Y ratio. But in case of plate (D), (U_z) the decreased with increase of D/Y. The variation of the deflections (U_{sum}), with respect to D/Y ratio, in orthotropic plates is more than that of isotropic plates for all boundary conditions. It is also observed that the trend of variation of deflection (U_{sum}) with D/Y ratio is almost the same for all materials for respective boundary conditions. For plate (A) the maximum shear stress was occurred in the XY plane, (τ_{xy}), and the minimum shear stress was occurred in YZ plane, (τ_{yz}). The shear stress in XZ plane (τ_{xz}) varied significantly with respect to D/Y ratio for both materials. For plates (B), (C) and (D), the maximum shear stress was occurred in the XY plane (τ_{xy}) and the minimum shear stress occur in XZ plane (τ_{xz}). The shear stress in YZ plane (τ_{yz}) varied significantly with respect to D/Y ratio for both materials. It is also observed that the variation of SCF for all stresses with D/Y ratio; highly depends on the elastic constants and differs with material to material. For all materials, the stresses were occurred at maximum values in plates(C) and (D) and at minimums in plates (A) and (B), Hence the SCF for σ_x and σ_y plays an important role in design of plates (C) and (D) and a minor role in the design of plates (A) and (B).

9. REFERENCES

1. X.J., Cheng, Wu. A higher order theory for plane stress conditions of laminates consisting of isotropic layers. *Journal of Applied Mechanics* 66 ,95–100, 1999.
2. C., J., Hsu, Chen. The stress intensity factors of slightly undulating interface cracks of bimetals. *International Journal of Fracture* 80, 277–293, 1996.
3. X.,F., Wang, Hasebe, N. Bending of a thin plate containing a rigid inclusion and a crack. *Engineering Analysis with Boundary Elements* 24, 145–153, 2000.
4. R. A. Chaudhuri, Stress concentration around a part through hole weakening laminated plate, *Computers & Structures*, vol. 27(5), pp. 601-609, 1987.
5. H., Y., Kohno, Ishikawa. Analysis of stress singularities at the corner point of square hole and rigid square inclusion in elastic plates by conformal mapping. *International Journal of Engineering Science* 31 (8), 1197–1213, 1993.
6. T. K. Paul, and K. M. Rao, Stress analysis in circular holes in FRP laminates under transverse load, *Computers & Structures*, vol. 33(4), pp. 929-935, 1989.

7. T. K. Paul, and K. M. Rao, Finite element evaluation of stress concentration factor of thick laminated plates under transverse loading, *Computers & Structures*, vol. 48(2), pp. 311-317, 1993.
8. B. P. Shastry, and G. V. Raj Effect of fiber orientation on stress concentration in a unidirectional tensile laminate of finite width with a central circular hole, *Fiber Science and Technology*, vol. 10, pp. 151- 154, 1997.
9. X. Xiwu, S. Liangxin, and F. Xuqi, Stress concentration of finite composite laminates with elliptical hole, *Computers & Structures*, vol.57(1), pp. 29-34, 1995.
10. X. Xiwu, S. Liangxin, and F. Xuqi, Stress concentration of finite composite laminates weakened by multiple elliptical holes, *International Journal of Solids Structures*, vol. 32(20), pp. 3001-3014, 1995.
11. T. Iwaki, Stress concentrations in a plate with two unequal circular holes, *International Journal of Engineering Sciences*, vol. 18(8), pp. 1077-1090, 1980.
12. V. Ukadgaonker, and D. K. Rao, A general solution for stress around holes in symmetric laminates under plane loading, *Composite Structure*, vol.49, pp. 339-354, 2000.
13. K. Ting, K. T. Chen, and W. S. Yang, Stress analysis of the multiple circular holes with the rhombic array using alternating method, *International Journal of Pressure Vessels and Piping* , vol. 76, pp. 503- 514, 1999.
14. E., Pan, Yang, B., Cai, G., Yuan, F.G. Stress analyses around holes in composite laminates using boundary element method. *Journal of Engineering Analysis with Boundary Elements* 25, 31–40, 2001.
15. S. G. Lekhnitskii, *Anisotropic Plates*. Gordon and Breach, New York (1968).
16. Help of The ANSYS Program V12.0. (2010).